Paper submitted within the scope of the Master's Thesis
Master of Industrial Sciences
GROUP T - Leuven Engineering College - 2009-2010

Modular Integrated Battery Management System for Lithium-based Batteries

Jonas Lejeune*, Maxime Vincent*, Ing. Daan Nies, Ing. Jeroen Van Aken‡

*Master student Electronics-ICT, Intelligent Electronics, GROUP T - Leuven Engineering College, A. Vesaliusstraat 13, 3000 Leuven
‡Unit Information, GROUP T - Leuven Engineering College, Vesaliusstraat 13, 3000 Leuven, jeroen.van.aken@groept.be

Abstract

While lithium-based batteries are a popular choice in electronic appliances, they are also one of the best options for use in electric vehicles. However, there are a few disadvantages holding back their advance. They are dangerous because of their sensitivity for over- and undervoltage, overcurrent and high temperature conditions. The objective of this work is to propose a solution that allows safer usage of these batteries. To achieve this goal an electronic circuit has been designed that keeps track of voltages, temperatures and currents and allows active balancing to prevent and anticipate possible faulty conditions. The circuit was tested individually in a lab environment and in the field in a solar car. Lab testing helped debugging the software and proved the robustness of the hardware. In the field testing revealed some additional problems that should be taken into account for further development.

Keywords— Active Balancing, Battery Management, Lithium Batteries, Solar Car

1 Introduction

1.1 Nature and scope of the problem

Lithium-based batteries have successfully been used for many years in all kinds of portable electronic appliances, e.g. cell phones, notebooks, GPS receivers, MP3-players... These batteries have some very important advantages over classic battery technologies, such as nickel-cadmium, lead-acid and nickel-metal-hydride. Firstly, lithium-based batteries have a higher energy density by volume and by mass. Secondly, they don't suffer from the memory effect (Linden & Reddy, 2002), they have a low self-discharge rate and a low internal impedance. Furthermore, they can be constructed in a prismatic as well as a cylindrical shape which provides the best fit for all applications. This makes lithium-based batteries an emerging choice for all kinds of electric vehicles even though there are a couple of disadvantages holding back their advance. They are dangerous because of their sensitivity for over- and undervoltage, overcurrent and high temperature conditions. If overheated or if charged to an excessively high voltage, they may suffer from thermal runaway and cell rupture. This may, in extreme cases, lead to incendiary and explosive effects. Furthermore, they may be irreversibly damaged when they are discharged below a certain treshold voltage (Buchman, 2001). That is exactly why balancing the cells in a battery pack allows to use the pack to it's full extend. When all cells are kept in an identical State-of-Charge, a bigger percentage of the pack capacity can be used, without damaging the cells. Otherwise upper or lower limits of one out-of-balance cell would form the upper charge or lower discharge limit for the whole pack, respectively.

Figure 1. The battery pack

The battery management system, or BMS, presented here is a solution that was designed to fit a 40S4P Lithium-polymer battery pack, shown in Figure 1. This consisted of 160 cells, of which 40 packs of 4 parallel cells, were placed in series and boasted a nominal voltage of 148 V and a capacity of 30 Ah, providing a total energy of approximately 4,5 kWh. The presented BMS was designed specifically for this pack, but with modularity kept in mind at all times. The objective of this work is to propose a solution that allows safer and more efficient use of these batteries.

Thus, the requirements for the BMS are the following:

- To provide continuous voltage monitoring of every individual lithium cell.
- To provide continuous temperature monitoring of every individual lithium cell.

- To provide continuous current monitoring of the current through the whole battery pack.
- To provide an accurate state-of-charge indication.
- To provide an efficient way to balance the battery pack.
- To be adaptable to future solar car battery packs and to other applications as well.
- To be a realistic and affordable solution for future battery packs.

Two parts of the highly qualitative Philips Research Books Series collect resources in the field of batteries, battery management (H.J. Bergveld, 2002) and state-of-charge determination (Pop, Bergveld, Danilov, Regtien, & Notten, 2008). These books are used as a leitmotiv throughout the design process.

1.2 Results

All of the goals stated earlier have been accomplished by the proposed design. Accurate voltage, temperature and current monitoring are all provided on regular time intervals. Active balancing with a reasonable efficiency is achieved as well. A combination of the voltage and current measurements is used to get a reasonably accurate state-of-charge indication. The one-PCB-per-cell design was proven to be very modular and certainly adaptable to many kinds of other battery packs. The cost-per-cell is approximately €15, which is a modest investment for the given gain in safety and efficiency.

1.3 Conclusions

The designed system adds significant safety to the lithium-based battery pack. It is easy to operate and interact with through the CAN-bus. The design is modular, which makes it a perfect fit for a lot of different battery packs using different amounts and types of lithium cells. It was not designed to be a stand-alone system; any actions altering normal use of the battery pack have to be commanded by the physical operator; this allows maximum control, which was needed for the solar car application. It is easy to overcome this, by slightly adapting the firmware. Automated security can be added by adding some simple hardware, e.g. a contactor controlled by the BMS that can interrupt the output of the battery pack. During testing in noisy environments, some communication problems between different parts on the PCB were encountered, which could be solved by adding chokes on the communication lines.

2 Design Method

2.1 Design method

The design presented in this paper was not obtained at once. A combination of the V-model and the spiral model, also called iterative approach, were used (Wille & Vede, 2008). For the entire design, the V-model approach, as shown in Figure 2, consisted of first defining a functional block diagram based on the requirements and clearly stating the different subcircuits that were responsible for the different functions of the BMS. Secondly, all of these subcircuits were developed using the iterative approach: initially, basic functionality was to be achieved; afterwards, an increasing amount of details were taken into account to make these circuits more cost-effective and more efficient. Once the hardware circuitry was finished, the software design was defined and coded, also by using an iterative approach. This part of the design process is also called the top-down approach (Walters, 2009), this is then followed by a bottom-up approach consisting of: the verification of the software and hardware design, followed by the integration of the complete system and the verification and validation of it. Starting by designing the subcircuits, allowed for early testing and the use of fully working, fully tested subcircuits facilitated the integration process to obtain a complete system.

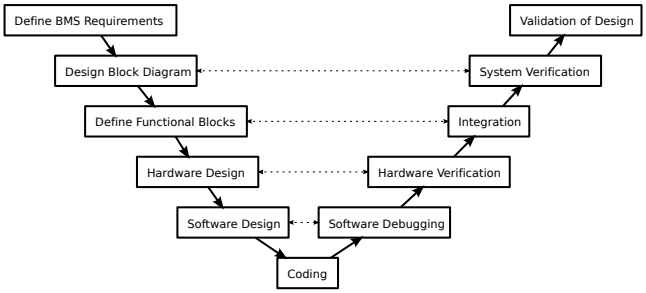

Figure 2. Design method: The V-model

2.2 Requirements

Existing battery management systems have the main drawback that they are made for a fixed number of battery cells. Often this number is too low for the battery pack of an electric vehicle, or a number of these systems have to be unconveniently linked together. Therefore we wanted to design a modular and easily scalable system that is suitable for any battery pack design ranging from a notebook up to an EV. The limitation of the number of series cells is mainly an I^2C addressing limitation, allowing up to 120 cells.

A battery monitoring system has to measure the individual cell voltages e.g. to allow the operator to take appropriate action when any of the cells tend to go out of balance or reach the voltage safety limits of the battery. Additionally, because of the sensitivity to temperature and the explosive character of lithium, it is also important to monitor the cell temperatures. In case something goes wrong and cells start to warm up, action can be taken before thermal runaway takes the cells up to dangerously high temperatures. For the same reasons, current should stay within the allowable limits of the battery cells.

The State-of-Charge (hereafter called SoC) is an indication of the amount of energy left in the batteries. When no load is attached to the battery, SoC can be determined by measuring the voltage. But under load conditions, the voltage drops related to the amount of load and the SoC must

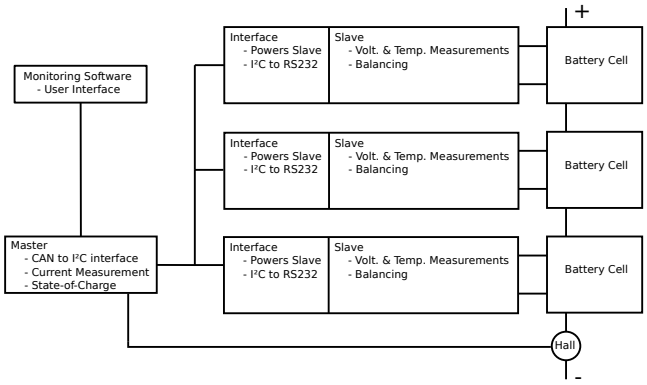

Figure 3. Functional diagram

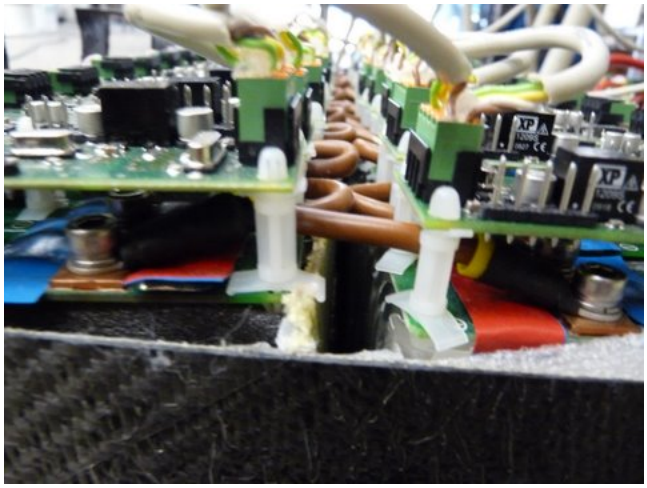

Figure 4. Battery PCB ↔ BMS-PCB spacer

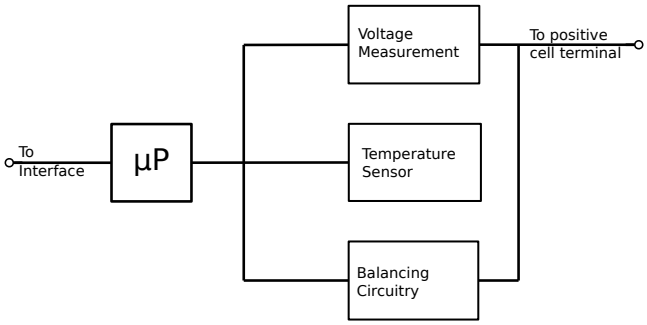

Figure 5. Functional diagram of the slave

be determined by measuring how much energy has left or entered the batteries. This is called coulomb counting and is done by integrating the current flowing in or out of the battery pack over time.

To extend the system from a monitoring system to a management system and to increase the efficient use of the batteries, a way must be provided to balance the batteries. When one of the cells becomes undercharged in comparison to the others, this cell forms the lower limit for the entire pack and vice versa when one of the cells becomes overcharged. To circumvent this problem, the cells must be balanced which increases the effective capacity of the pack. The most commonly used method to do this, is by discharging all the cells that have a higher voltage than the lowest charged cell(s). Since this obviously is a waste of energy, an active balancing system is required. Instead of discharging the highest cells, the lowest cells are charged; the energy used to charge these lowest cells comes from the entire battery pack and thus the energy of the whole pack is redistributed over all the cells.

3 Hardware Design

3.1 Result of the design process

3.1.1 BMS-PCB

The proposed design uses one BMS board per series battery cell and one master board for the entire battery pack. As a result, scalability is obtained: Any number of series cells can be used in a battery pack, as it is sufficient to add an extra BMS board for every extra series cell. Additionally, this allows to make a design for one cell and simplifies the design process. To electrically isolate the battery cells from each other, the PCB was split into two parts: A slave that does the measurements and controls the balancing circuitry and which shares the battery cell minus pole as ground; and an interfacing part that translates the commands for the slave and is isolated from the battery cell poles. The master board is the main controller in the battery pack and controls all the BMS boards on every series cell and it does the current sensing as well. An overview of this structure is shown in Figure 3. An electronic schematic of the entire circuit can be found as an appendix.

The physical mounting of the PCBs on the battery pack is done using five nylon spacers as can bee seen in Figure 4. Each battery cell in the employed battery pack, consists of four parallel soldered cells. A single, bigger cell could have been used, but this was not done because of the dimension constraints imposed on the battery pack in the solar car. A PCB on top of these four cells connects them in parallel. The BMS board is connected on top of this PCB, using nylon spacers to safely separate them from each other. Connection to the BMS is established using a four-pin connector providing two separate measuring and two balancing wires from the battery cell to the BMS. That way measurements are not influenced when balancing currents are running through their separate wires. An additional advantage of these nylon spacer lies in their damping property. This can be seen in the endurance test results in section 5.1

3.1.2 Slave

The slave is by far the most important part of the battery management system and can be seen schematically in Figure 5. The slave part of the BMS board is electrically isolated from the interface and master and thus from the CAN bus. It works on the same ground as the negative pole of the lithium cell because voltage measurement is performed by the slave, as is the individual cell balancing. The heart of the slave is

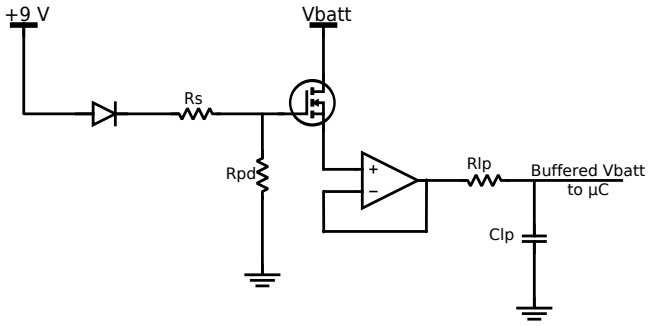

Figure 6. Voltage sensing circuit

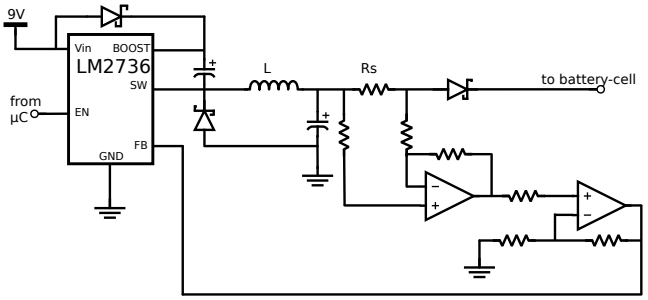

Figure 7. The balancing circuitry

a Microchip PIC18F2221. This is a powerful and relatively cheap 8 bit microcontroller. It has features such as: nanowatt power modes to reduce power consumption, an integrated 10 bit analog-to-digital converter, hardware support for I^2C and UART and is C-programmable which facilitates rapid development (Microchip Technology Inc., 2009b). The slave is powered by an individual DC/DC converter, which on its turn is powered by the 12 V of the CAN bus and provides an isolated 9 V supply for the entire slave. An input and output capacitor are used to limit both input and output transients and ripple. The chosen DC/DC converter is an IL1209S and combines high efficiency with a high cost-effectiveness (XP Power Ltd., 2009). To power the microcontroller and some sensors, a low-dropout regulator is used to generate a stable 5 V supply.

The voltage measurement is done using the analog-to-digital module of the microcontroller. This module has a 10 bit accuracy and the possibility to use voltage references as upper and lower bound. For the upper voltage reference, the low-dropout regulator is used. This is possible because of the very small output voltage tolerance, which gives an accuracy of ± 1 % and an excellent output voltage line regulation which is in the worst case 0,032 %/V over the full temperature range (National Semiconductor Corporation, 2007). The lower voltage reference consists of a 2,5 V precision voltage reference with an accuracy of ± 1 % and an output voltage line regulation of 0,035 %/V at worst over the full temperature range (Microchip Technology Inc., 2005). A typical lithium battery cell has a lower voltage of 2,7 V and and upper voltage of 4,3 V at most. Therefore using a lower voltage reference of 2,5 V instead of 0 V and an upper voltage reference of 5 V doubles the precision of the ADC measurement. This results in a resolution of 2,44 mV with a worst case uncertainty of 75 mV on the measurements. The voltage sensing occurs over two separate sensing wires. To prevent latch-up of the components of the slave by powering their in- or outputs while powered off, a MOSFET is used to connect the positive battery terminal to the measuring circuit. The gate of this MOSFET is turned on when the DC/DC that powers the slave is turned on; whenever the DC/DC is off, the gate is pulled to ground to prevent any current drain. The output of this MOSFET is buffered to reduce the voltage drop over the MOSFET, improving the accuracy of the measurement, as can be seen in Figure 6. This buffer also separates the AD-conversion from the balancing circuit to maintain correct AD-readings. To minimize the interferences of high frequency noise picked up on the trace to the microcontroller, a low pass filter is used. This has a cut-off frequency of 1850 Hz which is sufficiently low to remove any high frequency interferences and sufficiently high to easily let pass the voltage fluctuations. A first order RC-filter is used because of its low cost and a steep attenuation is not required.

To carry out the temperature measurement, an on-PCB MCP9700A temperature sensor was used. This sensor is optimized for use with the AD-converter of the microprocessor and is able to measure the temperature with an absolute accuracy of ± 2 °C and relative temperature changes of ± 1 °C (Microchip Technology Inc., 2009a). This mediocre accuracy is sufficient for the given application; namely monitoring that the battery pack temperature is staying within safe operation limits for the used lithium-cells. In the case of the cells used in the solar car this was 0 - 60 °C. This sensor was chosen because it is a linear active thermistor and thus does not need any additional signal conditioning. This results in reduced costs and less required PCB surface. In addition, this simplifies the conversion of the analog voltage to actual temperature. This sensor is able to drive large capacitive loads, which makes it immune to the effects of parasitic capacitances. The same low pass filter as used for the voltage measurement is also used here to minimize the effect of high frequency interference. The capacitance of this filter also helps to reduce over- and undershoots and thus improves the transient response when turning the slave on and off.

The balancing of the batteries requires a constant current for optimal performance. The balancing current in this application is approximately 300 mA. Based on the capacity of the cells of the solar car application of 30 Ah per cell, a balancing current of 0,3 A allows one cell to be charged for approximately 1 %, when charged during one hour. The LM2734, a monolithic switching step-down regulator, forms the heart of the current source (National Semiconductor Corporation, 2005). This switcher has a high efficiency, limits the number of required external components and hence reduces the required PCB surface and cost. The LM2734 in fact is meant to be used as a voltage source. The output should be connected with a simple voltage divider to the feedback pin, which allows the choice of the output voltage. To use it as a current source, the voltage over a 100 mΩ-shunt

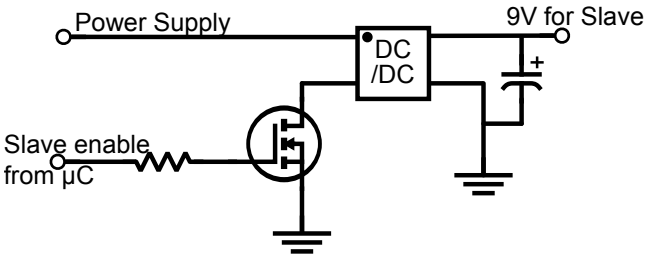

Figure 8. Slave power supply

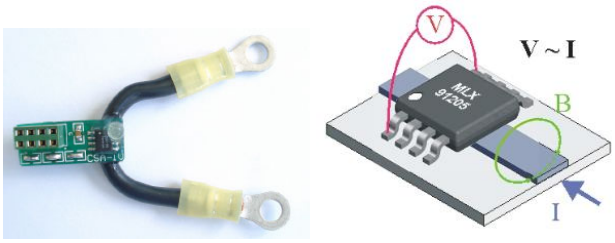

(a) Mounted sensor (b) Sensor principle

Figure 9. Melexis current sensor

resistor connected to the output is sensed and hence current is measured, instead of voltage. Proper scaling is done by a differential amplifier and a non-inverting amplifier. The output of these amplifiers is fed back to the feedback pin. This schematic is shown in Figure 7. The switching frequency of the LM2734 is 550 kHz. The Gain-Bandwidth-Product (GBP) of the amplification and bandwidth required for the feedback circuitry is too high to be handled by one amplifier. This issue is easily dealt with by splitting the amplification in two steps, thus gaining a lot of bandwidth. The required GBP is about 30 MHz and the employed LM6134 op-amps only guarantee a GBP of 7 Mhz. By splitting the amplification in two steps, we only require a GBP of approximately $\sqrt{30}$, staying safely under this limit. To calculate this GBP, we use a bandwidth of 1,1 MHz, which is two times the switching frequency of the switcher. The high switching frequency allows the use of a small surface mount inductor and chip capacitors. In this application this results in an inductance of 47 μH[1] with a very small footprint of only 6,6 mm by 6,6 mm. The saturation current is 1 A at a 30 % drop of inductance. This is necessary since the switcher can deliver transient currents up to its maximum rating, 1 A. A very low forward voltage drop Schottky diode is used as freewheeling diode to minimize power loss over this diode (Philips Semiconductors, 2005).

If we take a closer look at the efficiency of the balancing circuitry, it is obvious that there are a lot of step-down conversions we have to take into account. The power used to balance the cells is derived from the 12 V-line of the CAN-bus using the DC/DC that powers the slave-part of the BMS. This 12 V is generated using a higher-voltage DC/DC from the main power bus, which varies between 108 V and 168 V in our battery pack design. When the efficiencies of these individual conversions are added up, an overall balancing efficiency of > 60 % is reached as can be seen in (1).

$$\eta_{160V\to12V} \cdot \eta_{12V\to9V} \cdot \eta_{switcher} = 0,87 \cdot 0,82 \cdot 0,90 = 0,642 \quad (1)$$

3.1.3 *Interface*

The interface is a separate part on the BMS PCBs that operates on the same ground as the CAN-bus. This circuitry provides an interface between the only master in the entire battery pack and the slave on every BMS-board, as shown in Figure 3. Communication between the master and interface is established via the I^2C-bus. All BMS-boards in the battery pack, are connected to this same I^2C-bus. The master chooses the BMS-board to communicate with, sends its commands via I^2C and the interface contacts the slave via UART if needed, depending on the command sent. To ensure proper timings during communication this microcontroller uses a 10 MHz cristal as a clock source; for this reason the slave uses the same crystal as external clock source.

Because of the different grounds on the interface, which uses the ground supplied by the CAN-bus and the slave, which uses the ground of the battery cell; the communication lines have to be isolated. A digital isolator delivers high speed communication possibilities, facilitates the design compared to optocouplers and consumes only one-tenth to one-sixth the power of an optocoupler at a comparable data rate (Analog Devices, 2009). The chosen ADuM1201 isolator provides an isolated transmitting and a separate, equally isolated receiving channel.

Another feature of this interface is the ability to power on and off the slave-part of the BMS-board, therefore it saves power when no measurements need to be done and no cells have to be balanced. This is done by switching the path to ground of the isolated DC/DC converter of the slave-part through a MOSFET as shown in Figure 8.

3.1.4 *Master*

The master is a separate PCB and an independent CAN-node in the solar car. It provides the interface between the battery management system's PCBs on each cell and the rest of the CAN-network. All commands from the operator are given through the CAN interface and are interpreted by this node. See Figure 3 for a better understanding. Consequently, appropriate action is taken. This master is also responsible for polling the BMS-boards to request their data, which takes place every 10 s in the given application (every 250 ms another BMS is queried).

Another role consists of the current measurement. This is accomplished by a Melexis MLX91205 HALL Effect current sensor, as shown in Figure 9(b), which is capable of measuring current from DC up to 100 kHz. The linearity is excellent, since it was calibrated for our specific application by Melexis technicians. (Melexis NV, 2009). One sensor of this type is mounted on a battery cell interconnection

[1]Calculations can be found in appendix.

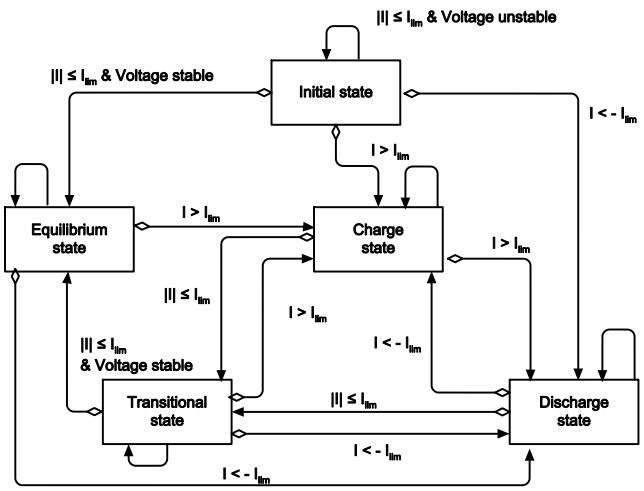

Figure 10. Finite state model of the SoC-algorithm

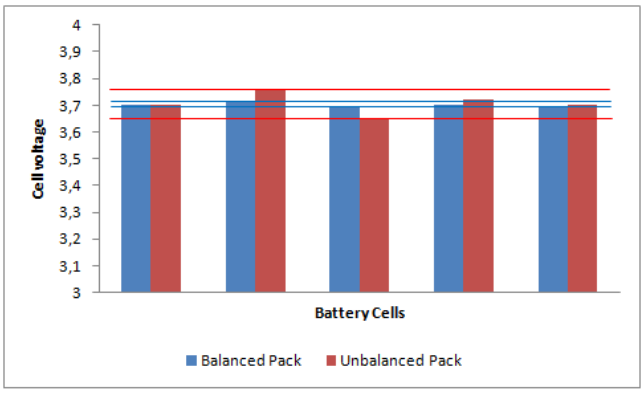

Figure 11. Comparison between balanced and unbalanced batterypacks

cable, see Figure 9(a), measuring the current between two cells and hence the current through the whole battery pack. This information is put on the CAN-bus, but is also used for State-of-Charge determination. It is sampled on a regular time-basis, allowing to integrate current over time, therefore yielding the electric charge that was put in or pulled out of the batteries. The SoC algorithm is explained hereafter, in the software section 4.1.1.

4 Software Design

4.1 Implementation

As all microcontrollers are from the PIC18F-series from Microchip, all code for the firmware was written in C. This allows rapid prototyping and simplifies the design process while making it possible to make rapid changes when deemed necessary during the testing.

4.1.1 State-of-Charge algorithm

The SoC-algorithm is loosely based on a method presented by H.J. Bergveld (Pop et al., 2008). The algorithm is a basic finite state machine that evaluates the inputs to determine the correct method to calculate the State-of-Charge. In the initial state, see Figure 10, the SoC is calculated based on the cell voltage and a stored relationship between the SoC and the Electro-Motive Force (EMF). This relationship is accurate as long as there is no current flowing. Depending on wether the batteries are being charged, discharged or in equilibrium, the state machine will move to the appropriate state.

The equilibrium state is reached when almost no current is drawn from or flows into the batteries. The limiting current which defines the borders of this state is defined in the system, based on the capacity of the batteries. At this very low current, the battery voltage is very close to the EMF value, providing that the voltage is stable. Therefore, in this state the determination of the SoC is based on the stored SoC-EMF relationship again.

In the charge and discharge state, a current larger than I_{lim} flows respectively in or out the batteries; the SoC is calculated by Coulomb counting. This involves the use of the previously determined SoC and the amount of energy that left or entered the batteries to update the current SoC.

After passing through the charging or discharging state, the algorithm always passes the transitional state before the equilibrium state is reached again. The purpose of this transitional state is to determine whether the battery voltage is stable and the algorithm is allowed to enter the equilibrium state. As long as this is not the case, the SoC is determined using Coulomb counting, as in the charging and discharging state. As soon as the battery voltage is stable and the current is still less than the limiting current, the algorithm enters the equilibrium state.

The main advantage of this algorithm is that an accurate SoC can be determined using low-cost hardware and commonly available microcontrollers.

4.1.2 Balancing algorithm

The determination of the cells to be charged, can be done manually by the operator or automatically by the balancing algorithm. This algorithm is, just like the SoC-algorithm, executed on the master. The master collects the data from all individual BMS-boards and calculates the mean cell voltage. The lowest cell voltage is then compared to this mean voltage and if it is a certain threshold voltage lower than the mean voltage, the balancing operation is started for the lowest cells. This is done by sending a message to the respective interface; these cells are then charged for a fixed amount of time, depending on their voltage difference with the mean voltage. Thereafter, all cell voltages are compared again and the balancing cycle is started over. This is repeated until all the battery voltages are within the set thresholds of the mean voltage or the operator stops the balancing algorithm. The maximum number of cells that can be charged at once is five, this constraint is imposed to limit the current drawn from the 12 V line.

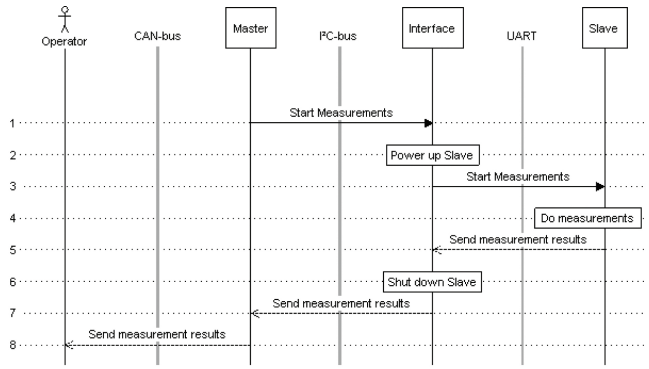

Figure 12. Sequence diagram of the measurement-communication

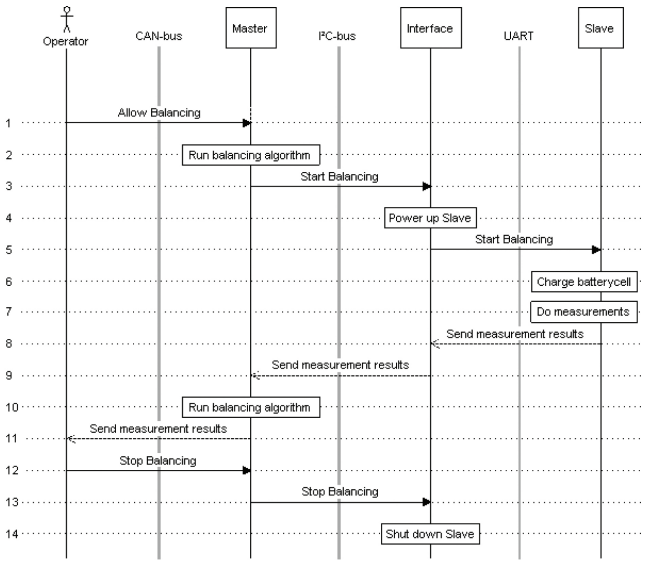

Figure 13. Sequence diagram of the balancing-communication

4.2 Operation

4.2.1 Course of communication

The sequence of the communication is shown in Figure 12. The measurement cycle starts automatically when the BMS is powered; the master polls all the BMS-boards individually every 10 s (one board is shown in the diagram, every 250 ms another board is thus polled). On receipt of the "start measurements"-command, the interface powers the slave by enabling the MOSFET that switches on the DC/DC converter that power the slave (as discussed in section 3.1.3). After a hold-off period to allow the slave to boot up, the interface translates the "start measurements" command to the UART-communication line of the slave. The slave then starts to perform all measurements by reading its sensors (as described in section 3.1.2). Once all measurements have been carried out, the slave sends the results to the interface, which translates them to the I^2C-bus to send the measurements to the master. The master stores these results for use in the SoC- and balancing-algorithm and sends them over the CAN-bus to the operator. The balancing follows a slightly different communication sequence, as shown in Figure 13. For balancing to be possible, the operator must first send the "allow balancing"-command to the master. Upon receiving this command, the master initiates the balancing algorithm that has been described in 4.1.2. The master controls this algorithm and stops the balancing when all cells seem to be in balance or when the operator decides to send the "stop balancing"-command. If the operator has manually selected the cells to be charged, the master stops the balancing when these cells reach the mean voltage.

4.2.2 CAN data

To communicate between the master and the operator, a CAN-bus is used; the format of a frame on this bus is shown in Figure 14(a) and more detailed in Table 1. Every CAN-frame consists of a header containing an 11-bit identifier, some control bits and the data-part; there is the possibility to use an extended identifier if more CAN-nodes are present but since this was not the case in our application, this will not be discussed. This identifier starts at a preset base address and is increased for each battery cell. This allows easy linking of the data to the right battery cells in the battery pack.

Field name		length (bits)
Header	Start-of-frame	1
	Identifier	11
	Remote Transmission Request	1
	Identifier Extension Bit	1
	Reserved Bit (R0)	1
	Data Length Code	4
Data Field		0-8 bytes
Cyclic Redundancy Check		16
Acknowledge		2
End-of-Frame		7

Table 1. Structure of a CAN frame

There are only a few different CAN messages used, these data frames are shown in Figures 14(b), 14(c) and 14(d). The status message contains the 10 raw bits from the ADC voltage measurement, representing cell voltage, the 8 bits from the ADC for the temperature measurement and a few status bits, these bits indicate for instance if the battery cell is being balanced. To transmit the SoC, two floating point values are encoded in two times four bytes of the data frame; the first represents the current SoC based on the SoC-algorithm and the second is the last SoC based on an open-circuit measurement. This last value is mainly for debugging of the SoC-algorithm.

The command to start balancing contains a flag to start automatic balancing and a byte to balance manually. When manual balancing is chosen, up to six battery-identifiers can be supplied by the operator which determines the particular cells to balance.

(a) Structure of a CAN message

(b) Status data frame

(c) SoC data frame

(d) Balancing data frame

Figure 14. The structure of the used CAN data frames

4.2.3 Monitoring software

The monitoring software has as goal to present all the data gathered by the BMS boards in a way that makes it easy for the operator to spot any potential risks in time and act accordingly. In our application, a bar-graph overview is used that shows all the batteries together with lines marking the maximum, the minimum and the mean-voltage. This way, the operator is able to see at a glance if any battery cells are getting dangerously out of balance. A screenshot can be seen in Figure 15. Besides the display of this information, the monitoring software can also initiate different actions, such as the starting or stopping of balancing, requesting to do measurements, ... This application is developed in Labview

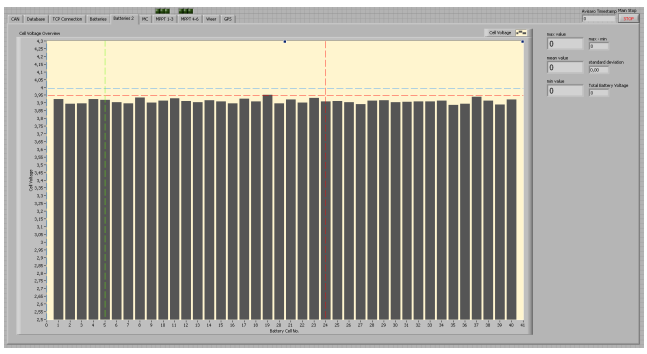

Figure 15. The monitoring software used to display all information to the operator

and serves as a monitoring application for all data gathered in the solar car. Further discussion about the design of this application is beyond the scope of this work.

5 Testing & Results

5.1 Endurance tests

To ensure proper operation in extreme conditions, the designed PCB was put under different tests at Jabil Circuit. These tests consisted of boot-up, continuous running and shut-down operations under different conditions. The goal was on the one hand to investigate how the PCB would behave under extreme conditions and on the other hand to search for the limits of the design.

The first series of tests consisted of a continuous decrease of the temperature, starting from room temperature. The microcontrollers were running when the temperature was decreased, then shut down and booted up again. Temperatures as far as -40 °C provided no problems for continuous running, booting up was only possible with higher temperatures, as far as -30 °C. After a resting period, this test was repeated with a continuously increasing temperature. This test demonstrated that the entire PCB worked flawlessly under temperatures up to 100 °C. At this temperature, the system would occasionally not boot up; this happened up to 120 °C at which point the system stopped working entirely. However, these limits were not fatal and although the PCB stopped working, there was no damage done such that when temperature was restored to room temperature, all functionality was recovered. The range in which the PCB is able to operate is thus rather large, this is because almost all components used were of industrial grade[2], except for the microcontroller which was not available at the time of design and could be the limiting factor. After the determination of these limits, a series of cycle tests were conducted, during which the temperature of the PCB would cycle between the most probable limits, which were 20 °C and 80 °C for this application. This cycle was repeated several times to ensure reliability in a fast-changing environment.

Besides temperature, humidity is another important environmental factor that can cause disturbance. In a specially provided humidity-chamber, the relative humidity was increased up to 80 % at a temperature of 80 °C. Because a humid environment can slowly damage electronic components, this test was conducted over a time frame of three days. After these days, no loss in functionality was detected and the operation continued. Since humidity is rarely mentioned in the datasheet, this test was the only way to be sure of proper operation under high relative humidity.

In the application of an electric vehicle, or more specifically a solar car, a third environmental factor that has to be taken into account is the possibility of sudden impacts. This was done by mounting the PCB on a special shaker as shown in Figure 16, in order to examine the effect of the nylon spacers (as described in 3.1.1), all these tests were carried out once with the PCBs mounted directly on the test bench and

[2]Industrially graded electronic components are guaranteed to work at temperatures ranging from -40 °C up to 85 °C.

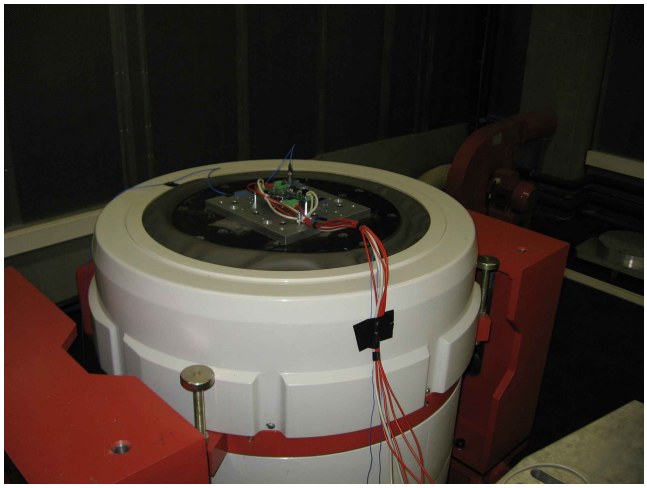

Figure 16. BMS mounted on shaker for shock testing

once using the spacers to mount the PCBs on the test bench. During these tests, the BMS was powered and functionality was verified using the CAN monitoring software. The first factor that was tested, was the ability of the PCB to withstand single shocks at different magnitudes. Tests were carried out at shocks of 5 and 10 G. Because single impacts are rare to happen in reality, further tests were done with random steps and sweeps of different shock pulses. The results of these tests can be found in the appendix and show that the PCBs have no physical problems with impacts and that the nylon spacers provide damping, reducing the effects of shocks on the BMS.

Although the hardware of our design showed no problems during these tests, some anomalies were unveiled on the software side. To stress the design, the software was configured for a high throughput; this required an optimization of the AD conversion parameters. The long test runs with high data throughput revealed that the software timings were not accurate enough and this occasionally lead to deadlocks. This was remedied by rewriting the software to be entirely interrupt driven to rule out possible deadlocks.

5.2 In the field usage

The first in the field tests have been carried out on the test track of Ford Belgium. In Australia, in Northern Territory, on the Cox Peninnsula Road, more extensive tests were conducted with satisfying results. These tests showed the importance of the extensive endurance testing done, as temperatures up to 50 °C were measured in the solar car. During these tests, the communication speed between the interface and the slave was lowered because it suffered from interference from the motorcontroller. The throughput of data to the CAN bus was also lowered to prevent congestion.

6 Discussion

The designed system adds significant safety to a lithium-based battery pack, whenever it is operated correctly. This means it is not completely fail-safe, because human interaction is still required. It was not designed to be a stand-alone system; any actions altering normal use of the battery pack have to be commanded by the operator through the CAN-bus. Or, if more severe, the system must be shut down manually, by the driver of the solar car in this specific application. This allows maximum control to the operator and driver. It is easy to overcome this, by slightly adapting the soft- and hardware. Over- and undervoltage protection and overtemperature protection can be provided by simply operating a contactor from the master. Pack balancing can be programmed to start automatically on a regular basis, if evaluated necessary.

The battery pack we used was of great quality; due to this, the disbalance of the cells was very limited. Only slight adjustments were needed and hence our charging current proved to be sufficient. There were no real long-term endurance tests (more than several months or even years of uninterrupted use) executed. It is possible that when the batteries start to age, the disbalance increases and therefore a higher balancing current could be more appropriate.

The design is modular, which makes it a perfect fit for many different battery pack configurations using various amounts and types of lithium cells. Clearly, the presented design offers a lot of flexibility in the amount of series cells. Using the 7 bit I^2C addressing, this could be from a single cell up to 120 series cells. 10 bit I^2C addressing could even be used, if 120 series cells form a limitation. However, the balancing circuit is now calculated for 30 Ah cells, and should work fine for anything between 10 and 40 Ah. What about bigger or smaller cells? More flexibility could be added by implementing the balancing circuitry as a separate plug-in PCB, to be mounted on the BMS boards. That way, different balancing PCBs can be made, for different cell capacities. Other limiting factors that should be taken into account when consindering more than 120 cells are the maximum isolation voltage of the ADuM digital isolator, the (longer) interval the slaves are getting polled and therefore the congestion of the I^2C bus.

An improvement to the reliability of the communication can be achieved by adding common-mode chokes to the communication lines. This is especially true in automotive applications where a lot of EMI is emitted by electronic control units, such as solar panel-trackers and the motorcontroller. EMI picked up by the data-lines can be filtered, thus limiting unwanted high-frequency noise on the bus and improving the susceptibility of the transceiver to electromagnetic disturbances. (Zeltwanger, 2008)

The method used to calculate the State-of-Charge is not the most accurate method possible, especially over longer time periods since we don't take self-discharge and battery-aging into account. However, due to the short lifetime of our specific application (a solar car designed for a single race of $\pm$3000 km), these factors were negligible and the used state-of-charge method proved to be more than sufficient. For applications with a longer lifetime, a more advanced State-of-Charge algorithm, such as adaptive filters described in (Pop et al., 2008), should be used; the disadvantage of these algorithms is their increased complexity and implementation

cost.

The overall efficiency of the balancing system could be improved in many ways. By upgrading the circuit to use a MOSFET with the gate connected to the enable pin of the switcher instead of the series diode, the forward voltage drop losses of the diode are circumvented. By using a different topology where the 12 V to 9 V DC/DC convertor is omitted and the switcher is powered directly from the 12 V line, the total efficiency goes up with > 15 %. We did not incorporate this in our design because of the practical implications this would have on the CAN-topology of the solar car.

The cost-per-cell is approximately €15, which is certainly acceptable for the gain in safety and efficiency provided by the BMS. Nevertheless, further cost reduction is possible by further stripping down the design to lower-range microcontrollers, cheaper DC/DC converters and by producing in higher quantities. That way a really cost-effective solution is obtained.

7 Appendix

Appendix A Calculations

Appendix B Schematics

Appendix C Used components

Appendix D Lithium batteries

Appendix E Endurance tests

8 Acknowledgements

During the design and building of this system, we received a lot of help without which we couldn't have gotten as far as we got. First we would like to thank Jeroen Van Aken for his inspiration and technical help.

Many of the people who helped us with this project, did this in the scope of a sponsorship to the Solar Team. Renaat Debaene and Jan Derde from PsiControl have provided us with insights in power electronics and practical design help that saved us a lot of time by warning us for possible pitfalls. Thanks to electronic equipment of Agilent, kindly provided by Gerbert Ruitenberg and Dominique Dubois, we were able to do our design and testing. Willy Serneels and Didier Desmet from Phoenix Contact helped us selecting, and provided us with the necessary connectors for the BMS. The testing at Jabil was a very informative experience, thanks to the help and patience of Patrick Achten.

A special thanks goes out to all the members of the Umicore Solar Team, with whom we designed and build the Umicar Inspire. They provided the necessary support and feedback during the development. In particular Bert Schuyten, who designed the CAN board that served as the master board for the BMS; and Ken Foncé who was responsible for the monitoring application.

At last we want to thank everyone who helped proofreading this paper to correct spelling and grammatical errors, in particular Sascha Buttgereit, Dorien Schrijnemakers and Stéphanie Jansen.

9 References

Analog Devices. (2009). *Dual-channel digital isolators ADuM1200/ADuM1201.* U.S.A.. Available from http://www.analog.com/static/imported-files/data_sheets/ADuM1200_1201.pdf

Buchman, I. (2001). *Batteries in a portable world: A handbook on rechargeable batteries for non-engineers* (2nd ed.). Vancouver, Canada: Cadex Electronics, Inc. Available from http://www.buchmann.ca/

H.J. Bergveld, W. K. P. N. (2002). *Battery management systems: Design by modelling* (1st ed., Vol. 1). Netherlands: Kluwer Academic Publishers.

Linden, D., & Reddy, T. B. (2002). *Handbook of batteries* (3rd ed.). New York, U.S.A.: McGraw-Hill.

Melexis NV. (2009). *MLX91205 IMC current sensor (triaxis technology).* Belgium. Available from http://www.melexis.com/Asset/Datasheet_MLX91205_DownloadLink_5505.aspx

Microchip Technology Inc. (2005). *MCP1525/41, 2.5V and 4.096V voltage references.* U.S.A.. Available from http://ww1.microchip.com/downloads/en/DeviceDoc/21653b.pdf

Microchip Technology Inc. (2009a). *MCP9700/9700a, MCP9701/9701a low-power linear active thermistor™ ICs.* U.S.A.. Available from http://ww1.microchip.com/downloads/en/DeviceDoc/21942e.pdf

Microchip Technology Inc. (2009b). *PIC18F2221/2321/4221/4321 family data sheet.* U.S.A.. Available from http://ww1.microchip.com/downloads/en/DeviceDoc/39689f.pdf

National Semiconductor Corporation. (2005). *LM2734 thin SOT23 1A load step-down dc-dc regulator.* U.S.A.. Available from http://www.national.com/ds/LM/LM2734.pdf

National Semiconductor Corporation. (2007). *LP2985 micropower 150mA low-noise ultra low-dropout regulator.* U.S.A.. Available from http://www.national.com/ds/LP/LP2985.pdf

Philips Semiconductors. (2005). *PMEG2005AEV very low V_F mega schottky barrier rectifier.* Netherlands. Available from http://www.nxp.com/documents/data_sheet/PMEG2005AEV_3005_4005.pdf

Pop, V., Bergveld, H., Danilov, D., Regtien, P., & Notten, P. (2008). *Battery management systems: Accurate state-of-charge indication for battery-powered applications* (Vol. 9). London, United Kingdom: Springer Verlag. Available from http://doc.utwente.nl/64893/

Walters, S. (2009). *Perl design patterns* (1.298 ed.). U.S.A.. Available from http://www.perldesignpatterns.com/

Wille, E. D., & Vede, D. (2008). *Software process models.* Schmidmühlen, Germany. Available from

http://www.the-software-experts.de/e_dta-sw-process.htm

XP Power Ltd. (2009). *DC-DC 2 watt IL series.* Singapore. Available from http://www.xppower.com/pdfs/SF_IL.pdf

Zeltwanger, H. (2008). *Common-mode chokes can cause transients in automotive CAN components.* Germany. Available from http://www.automotivedesignline.com/showArticle.jhtml?articleID=211600502